REPORT DOCUMENTATION PAGE

Form Approved
OMB No. 0704-0188

1. REPORT DATE *(DD-MM-YYYY)*	2. REPORT TYPE	3. DATES COVERED *(From - To)*
18-11-2011	Conference Proceedings	

4. TITLE AND SUBTITLE
Quantifying Turbulence Microstructure for Improvement of Underwater Imaging

5a. CONTRACT NUMBER

5b. GRANT NUMBER

5c. PROGRAM ELEMENT NUMBER
0602782N

6. AUTHOR(S)
Sarah Woods, Weilin Hou, Wesley Goode, Ewa Jarosz, Alan Weidemann

5d. PROJECT NUMBER

5e. TASK NUMBER

5f. WORK UNIT NUMBER
73-6369-01-5

7. PERFORMING ORGANIZATION NAME(S) AND ADDRESS(ES)
Naval Research Laboratory
Oceanography Division
Stennis Space Center, MS 39529-5004

8. PERFORMING ORGANIZATION REPORT NUMBER
NRL/PP/7330-11-0691

9. SPONSORING/MONITORING AGENCY NAME(S) AND ADDRESS(ES)
Office of Naval Research
One Liberty Center
875 North Randolph Street, Suite 1425
Arlington, VA 22203-1995

10. SPONSOR/MONITOR'S ACRONYM(S)
ONR

11. SPONSOR/MONITOR'S REPORT NUMBER(S)

12. DISTRIBUTION/AVAILABILITY STATEMENT
Approved for public release, distribution is unlimited.

20111214048

13. SUPPLEMENTARY NOTES

14. ABSTRACT
Enhancing visibility through scattering media is important in many fields for gaining information from the scattering medium. In the ocean, in particular, enhancement of imaging and visibility is important for divers, navigation, robotics, and target and mine detection and classification. Light scattering from particulates and turbulence in the ocean strongly affects underwater visibility. The magnitude of this degrading effect depends upon the underwater environment, and can rapidly degrade the quality of underwater imaging under certain conditions. To facilitate study of the impact of turbulence upon underwater imaging and to check against our previously developed model, quantified observation of the image degradation concurrent with characterization of the turbulent flow is necessary, spanning a variety of turbulent strengths. Therefore, we present field measurements of turbulence microstructure from the July 2010 Skaneateles Optical Turbulence Exercise (SOTEX), during which images of a target were collected over a 5 m path length at various depths in the water column, concurrent with profiles of the turbulent strength, optical properties, temperature, and conductivity. Turbulence was characterized by the turbulent kinetic energy dissipation (TKED) and thermal dissipation (TD) rates, which were obtained using both a Rockland Scientific Vertical Microstructure Profiler (VMP) and a Nortek Vector velocimeter in combination with a PME CT sensor. While the two instrumental setups demonstrate reasonable agreement, some irregularities highlight the spatial and temporal variability of the turbulence field. Supplementary measurements with the Vector/CT in a controlled laboratory convective tank will shed additional light on the quantitative relationship between image degradation and turbulence strength.

15. SUBJECT TERMS
turbulence, kinetic energy dissipation, thermal dissipation, acoustic Doppler velocimeter

16. SECURITY CLASSIFICATION OF:			17. LIMITATION OF ABSTRACT	18. NUMBER OF PAGES	19a. NAME OF RESPONSIBLE PERSON
a. REPORT	b. ABSTRACT	c. THIS PAGE			Weilin Hou
Unclassified	Unclassified	Unclassified	UL	11	19b. TELEPHONE NUMBER *(Include area code)* 228-688-5257

Quantifying turbulence microstructure for improvement of underwater imaging

Sarah Woods[1,2,*], Weilin Hou[1], Wesley Goode[1], Ewa Jarosz[1], Alan Weidemann[1]
[1] Ocean Sciences Branch, Naval Research Laboratory, Stennis Space Center, MS, 39529 USA
[2] NRL ASEE Postdoctoral Fellow

ABSTRACT

Enhancing visibility through scattering media is important in many fields for gaining information from the scattering medium. In the ocean, in particular, enhancement of imaging and visibility is important for divers, navigation, robotics, and target and mine detection and classification. Light scattering from particulates and turbulence in the ocean strongly affects underwater visibility. The magnitude of this degrading effect depends upon the underwater environment, and can rapidly degrade the quality of underwater imaging under certain conditions. To facilitate study of the impact of turbulence upon underwater imaging and to check against our previously developed model, quantified observation of the image degradation concurrent with characterization of the turbulent flow is necessary, spanning a variety of turbulent strengths. Therefore, we present field measurements of turbulence microstructure from the July 2010 Skaneateles Optical Turbulence Exercise (SOTEX), during which images of a target were collected over a 5 m path length at various depths in the water column, concurrent with profiles of the turbulent strength, optical properties, temperature, and conductivity. Turbulence was characterized by the turbulent kinetic energy dissipation (TKED) and thermal dissipation (TD) rates, which were obtained using both a Rockland Scientific Vertical Microstructure Profiler (VMP) and a Nortek Vector velocimeter in combination with a PME CT sensor. While the two instrumental setups demonstrate reasonable agreement, some irregularities highlight the spatial and temporal variability of the turbulence field. Supplementary measurements with the Vector/CT in a controlled laboratory convective tank will shed additional light on the quantitative relationship between image degradation and turbulence strength.

Keywords: turbulence, kinetic energy dissipation, thermal dissipation, acoustic Doppler velocimeter, vertical microstructure profiler, underwater imaging

1. INTRODUCTION

The capability to see farther underwater is of interest in many different fields, particularly in the field of underwater imaging. Enhancement of imaging and visibility is important for underwater photography, divers, navigation, robotics, archeology, and target and mine detection and classification. Common underwater imaging technologies include both passive and active sensors, and include techniques such as sonar, and electro-optics imaging. Each approach to imaging underwater has its advantages and limitations, and in the ocean these limitations can quickly become very restrictive. Many efforts have been made to overcome these limitations under different oceanic conditions, and it is this aim that motivates the work presented here, which seeks to improve underwater imaging under the limiting conditions of turbulence.

In order to enhance electro-optics underwater imaging, an understanding of the physics involved in light propagation underwater is necessary. As the light propagates through the water column, scattering degrades the quality of the image. This scattering may be attributed to a combination of sources: the water itself, particulates suspended in the water column, or turbulence present along the propagation path. The magnitude of this degrading effect depends upon the underwater environment, and can rapidly degrade the quality of underwater imaging under certain conditions [1]. While scattering from particulates contributes more significantly to image degradation in general, especially at larger viewing angles, under conditions of strong turbulence, as is found near the surface, mixed layer, and bottom of the water column,

*sarah.woods.ctr@nrlssc.navy.mil

Ocean Sensing and Monitoring III, edited by Weilin W. Hou, Robert Arnone, Proc. of SPIE Vol. 8030, 80300A · © 2011 SPIE · CCC code: 0277-786X/11/$18 · doi: 10.1117/12.887607

near-forward turbulent scattering produces a significant contribution [2, 3]. The work presented here therefore seeks to better quantify the degrading effects of scattering from turbulence upon underwater imaging. Such quantization will not only allow for improved understanding of the physics contributing to the degradation of underwater imaging, but will also provide opportunity for overcoming such degradation and opening the door to opportunities for enhancing imaging techniques. This effort will also provide insight into optical techniques for characterizing turbulent flow in the water column. As a part of this larger effort, the present paper details the turbulence measurements from a field experiment consisting of simultaneous acquisition of images and measurements of the turbulent strength over which the images were obtained. A companion paper in this proceeding, Ref. [4], discusses the implications of turbulence on underwater imaging, including results from the field exercise discussed here, in further detail.

2. BACKGROUND

It has long been acknowledged that turbulence affects propagation of light in the ocean [5-7]. Physically, this is because turbulent inhomogeneities of the flow are associated with fluctuations in temperature and salinity. Variations in these passive scalars alter the water density, inducing variations in the refractive index. These fluctuations in the refractive index then refract the light as it passes through the turbulent layer, effectively inducing multiple forward scattering in the light beam [5-8]. In many applications in ocean optics, the contribution of scattering from particles is of higher importance than that of turbulence due to the small angles at which turbulence scatters the light. In applications such as underwater imaging, however, the near-forward scattering from turbulence becomes a limiting factor over longer ranges and under conditions of stronger turbulence [8]. In general, the turbulent strength is characterized by the turbulent kinetic energy (TKED) and thermal (TD) dissipation rates. The TKED rate, ε, determines the size of the smallest structure within the flow, and may be determined by the spatial gradients of the velocity field. The TD rate, χ, describes the size of thermal variations across the smallest structure of the flow, and may thus be determined by the spatial gradient of temperature variations.

Theoretically, if the scattering properties of the medium can be well-characterized, so as to provide the point spread function (PSF), the degradation of underwater images due to scattering from particles and turbulence may be overcome through image restoration by means of deconvolution and super resolution [9]. An observed image may be described as the convolution of the signal from the original object with that of the scattering medium. The signal from the scattering medium is described by the PSF, which describes how a point source of light is scattered after propagating through the scattering medium. Based on this principle, work has been done, and proven successful, in implementing an algorithm to correct for the effects of scattering from particles [10-12]. These methods are more complicated for scattering from turbulence, however, due to the rapid temporal and spatial variation of the turbulence field, even within the field of view of the sensor. Thus, turbulence presents a more difficult problem. The behavior of scattering from particulates has received much more attention than that of turbulence, and thus the behavior of scattering from oceanic turbulence is not as well known. This challenge motivates the current work, which seeks to provide insight into the impacts and limitations of turbulence upon imaging systems.

3. FIELD SITE

The Skaneateles Optical Turbulence EXercise (SOTEX) was conducted on Lake Skaneateles, New York in July 2010 and consisted of optical and turbulent characterization of the water column, concurrent with acquisition of underwater images. Images were collected over a 5 m path length at various depths within the water column, and at different sites on the lake. Figure 1 shows the approximate location of the two stations, the first (S1, red circle) near the center of the lake (42.8668° N, 76.3920° W) over a sloping bottom with an approximate depth of 70 m, the second (S2, blue triangle) at the northern end of the lake (42.9063° N, 76.4058° W) over a flatter bottom with an approximate depth of 50 m. Skaneateles was chosen for this exercise on account of its well-known optically clean waters, having the highest clarity of any of the Finger Lakes, with an average secchi depth near 8 m [13], thus allowing for imaging under varied turbulent strength, but with little scattering contribution from particulates. July was chosen for this exercise to ensure a well-defined thermocline (as demonstrated by the temperature profiles shown in Figure 2) and strongest possible conditions for optical turbulence in the lake.

Turbulence measurements were obtained from both a Vertical Microstructure Profiler (VMP) and a Vector Velocimeter combined with a Conductivity and Temperature sensor (Vector/CT). For deployment on the first day (July 27th), the Vector/CT was deployed on the optics package, with the VMP deployed from a separate vessel, as depicted in Figure 3(a). While the Vector/CT profile consisted of pauses at particular depths for acquiring a time series of velocities that would be used for turbulence calculations, the VMP profiled continuously. For all subsequent days, the Vector/CT was deployed upon the IMAST (Image Measurement Assembly for Subsurface Turbulence), a 5 m long rigid structure used for acquiring images. The IMAST was deployed both vertically and horizontally, as depicted in Figure 3(b), both during the day with a passive imaging target and at night with an active target, and also profiled the water column in a step fashion, pausing at each depth for a given period of time to acquire images and velocity time series at a given depth. The VMP was deployed from a separate vessel in close proximity, and profiled continuously during the IMAST deployment. Complementary profiles of the water column optical properties were also obtained with a WETLab ac-9, bb sensor, CTD, and a Sequoia Scientific Laser In-Situ Scattering Transmissometer (LISST).

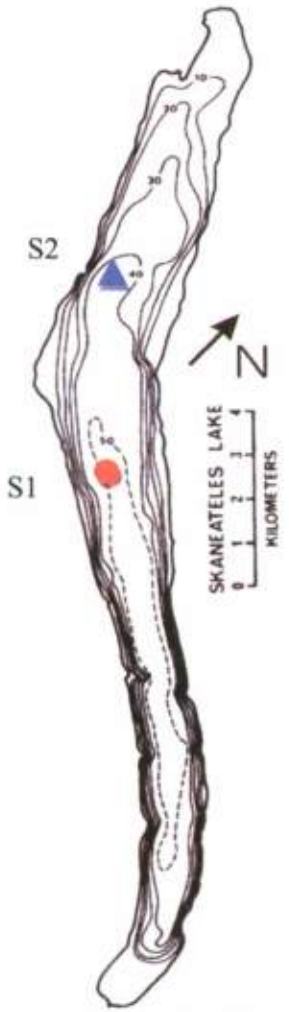

Figure 1. Bathymetric sketch of Skaneateles Lake showing the approximate location of the two stations: S1 (red circle) near the center of the lake, and S2 (blue triangle) in the northern end of the lake. Map adapted from http://www.ourlake.org/html.

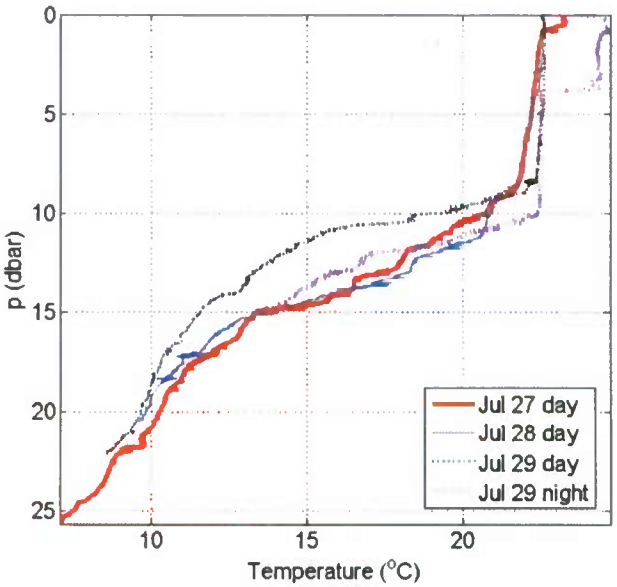

Figure 2. Temperature profiles (°C) corresponding to the dissipation profiles shown in Figure 5 for deployments on July 27 day (thick solid red), July 28 day (thin solid blue), July 29 day (thin dotted black), July 29 night (thick dotted purple). All profiles are from S1 except for the July 29th daytime deployment, which is from S2. Depth is indicated by pressure (dbar).

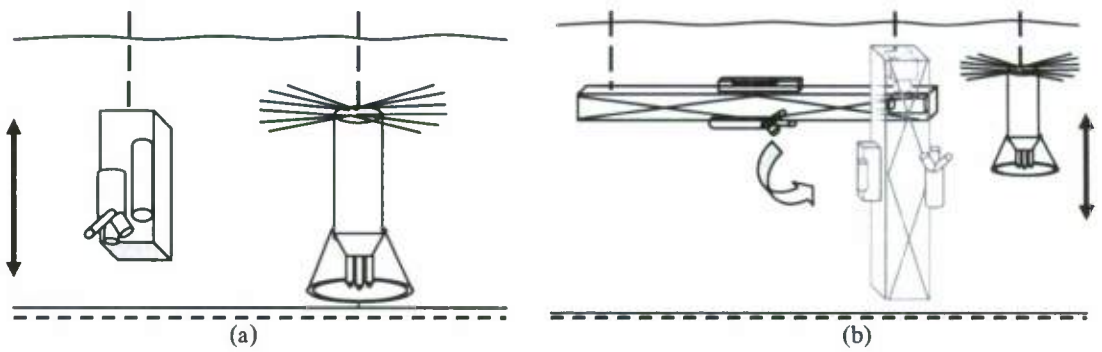

Figure 3. Diagram of deployment setup showing alternate deployment configurations: (a) Vector/CT (left) deployed vertically on optics package, and (b) Vector/CT deployed on IMAST (left) both vertically and horizontally. Note, in both instances, the VMP (right) was deployed from a separate vessel nearby.

4. TURBULENT DISSIPATION MEASUREMENTS AND CALUCATIONS

Two sets of instrumentation were utilized for characterizing the turbulence strength during SOTEX in order to provide a comparison between the background turbulence of the lake and the turbulence within the IMAST, to ensure the IMAST itself was not inducing significant turbulence. The current work will detail observations of the TKED rate, ε, from both instruments and the TD rate, χ, from the VMP. The first instrumental setup, the Vector/CT, consists of a Nortek Vector acoustic Doppler 3D velocimeter and a Precision Measurements Engineering (PME) fast Conductivity and Temperature (CT) sensor. The two instruments are mounted near the center of the IMAST structure, and the heads of the instruments placed in such a way as to sample the same volume of water, thus providing time series of the 3D velocity, temperature, and conductivity fluctuations of the sample water volume. As the instrument is commonly used for laboratory measurements or stationary moorings, the instrument requires collection of a time series of velocities at a stationary depth in order to compute the turbulent dissipation rates. Therefore, during deployment, the IMAST profiled

the water column by pausing at each depth for five to fifteen minutes to capture the turbulence statistics. Since the instrument was deployed from a vessel and not a stationary platform, the influence of the surface movement of the vessel was evident in some of the velocity spectra, however it did not affect dissipation estimates since its spectral signature was outside the inertial subrange used for calculations. Measurements were collected at a rate of 32 Hz to allow for adequate sampling of turbulent fluctuations.

The second instrument, providing microstructure observations for SOTEX, is a vertical microstructure profiler (VMP), designed and produced by Rockland Scientific International, Canada. The VMP profiler is designed to measure dissipation-scale turbulence in oceans and lakes up to 500 m. It is equipped with four microstructure sensors: two shear sensor probes, one thermistor (FP07), and micro-conductivity (SBE7) sensor. These sensors allow measuring with high accuracy and resolution microscale velocity shear, temperature, and conductivity, with a shear sampling rate of 512 Hz. Additionally, the VMP profiler has externally attached SeaBird SBE7-3F temperature and SBE-4C conductivity sensors. The profiler also measures pressure. During SOTEX, over 100 VMP drop profiles were executed, with drop velocities between 60 and 90 cm/s for estimating TKED, and drop velocities between 20 and 35 cm/s for estimating TD. All drops returned high-quality data that later were used to estimate turbulent energy and temperature dissipation rates from the shear and thermistor data, respectively.

4.1 Vector/CT and VMP turbulent kinetic energy dissipation

From the velocity measurements of the Vector, velocity spectra were computed from 10 minute long time series. This 10-minute period was chosen to meet stationarity of the turbulence statistics. Since the velocity spectra conform to a -5/3 slope over a wide frequency range, as shown by the sample spectra in Figure 4, the energy spectra relations used under the condition of local isotropy are applicable assuming Kolmogorov's theory. The TKED rate is then determined from

$$\varepsilon = \left[\frac{1}{C\alpha} k^{5/3} S(k) \right]^{3/2} \tag{1}$$

by fitting a line with a -5/3 slope to the inertial subrange of the velocity spectra. Here, k is the wavenumber, S the velocity spectral density, and C and α are constants given by 18/55 and 1.5, as determined from the isotropic relations and experimental results, respectively [14].

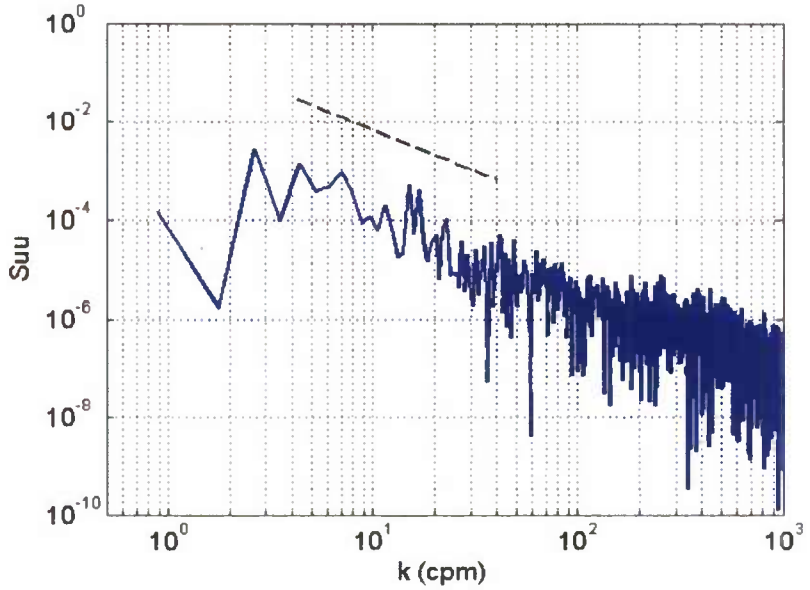

Figure 4. Sample velocity spectra from Nortek Vector Velocimeter (solid blue line), showing -5/3 slope (dashed black line).

From the VMP profiles, the TKED rate was computed by integrating the shear spectrum from k_1 to k_2 using the isotropic formula:

$$\varepsilon = \frac{15}{2}\nu \int_{k_1}^{k_2} \psi(k)dk \ , \tag{2}$$

where k is the wavenumber, ν the kinematic molecular viscosity of water, and $\psi(k)$ is the shear spectrum. Spectra of the velocity shear, like the sample one in Figure 5, were calculated from consecutive segments of 1024 data points, corresponding to a bin height of approximately 0.8 m, with an overlap between adjacent bins of 512 points. The lowest wavenumber, k_1, was set to 1 cpm, and the highest one, k_2, was set to the wavenumber where the shear spectrum has a minimum between the natural spectrum and a high wavenumber peak, but not higher than 30 cpm.

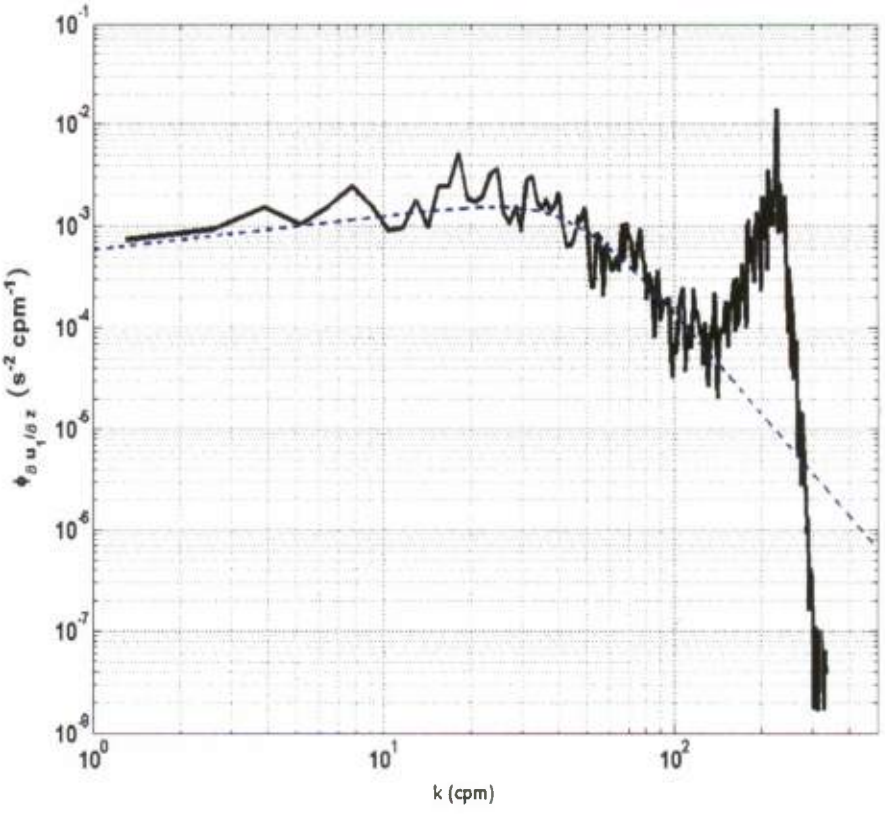

Figure 5. Sample shear spectra as measured with the Rockland Scientific VMP (black solid line) and fitted Nasmyth spectrum (dashed blue curve) for $\varepsilon = 6*10^{-7}$ m^2/s^3.

4.3 VMP turbulent thermal dissipation

The rate of loss of temperature variance is determined from microstructure measurements of temperature using very fast-response glass-enclosed thermistors. Assuming isotropy, the thermal dissipation rate, χ, was estimated from the following formula [15]:

$$\chi = 6D_T \overline{\left(\frac{dT'}{dz}\right)^2} \ , \tag{3}$$

where D_T is the thermal diffusivity, T' is the temperature fluctuation, and $\overline{\left(\frac{dT'}{dz}\right)^2}$ is the bin average of the squared gradient of the temperature variance in the vertical direction, z. An accurate determination of χ requires estimates of spatial temperature gradients with resolution to the Batchelor scale, which is beyond the capability of conventional sensors. Hence, interpolation was made for SOTEX observations by fitting the measured temperature gradient spectra determined over a limited wavenumber range to the universal Batchelor form of that given by Ref. [16]. The diffusive cutoff wavenumber, k_B, was taken as:

$$k_B = \left(\frac{1}{2\pi}\right)\left(\frac{\varepsilon}{\nu D_T^2}\right)^{1/4}, \tag{4}$$

where ε is the turbulent energy dissipation rate, and ν is the kinetic viscosity. Spectra of the temperature gradient were calculated from consecutive segments of 1024 data points with an overlap between adjacent bins of 512 points, corresponding to a mean bin height of approximately 0.45 m.

5. RESULTS AND DISCUSSION

From the relations given in the previous section, turbulent kinetic energy dissipation rates were determined from the Vector Velocimeter, and turbulent kinetic energy and thermal dissipation rates were determined from the VMP. While both instruments here provide results of turbulent dissipation in the form of profiles through the water column, it should be kept in mind that the VMP profiled continuously in order to provide dissipation estimates from the shear spectra, while the Vector/CT paused at a given depth in order to provide dissipation estimates from the velocity spectra at that depth. Comparisons of the dissipation rates for varying deployments are presented in Figure 6, where the Vector/CT TKED measurements are plotted as red open circles, and the VMP measurements are plotted as blue triangle (TKED rate) and black dots (TD rate). The results plotted in Figure 6(d) were collected during the nighttime deployment, but all other results are from daytime measurements. Similarly, the results in (c) were collected from station S2, but all other results are from S1. And finally, all results are from deployment of the Vector/CT mounted inside the IMAST except for (a), when it was deployed on the outside of the optics package. No measurements were made directly beneath the surface due to instrument deployment limitations of the VMP, but begin at a depth of about 5 m, and extend to depths of 40 to 60 m for the VMP, 15 to 25 m for the Vector/CT. Figure 7 shows VMP profiles of the (a) TKED and (b) TD rates, interpolated with depth and time to highlight the temporal and spatial variability of the turbulence field.

All profiles shown in Figures 6 and 7 generally depict heightened turbulent kinetic energy dissipation rates near the mixed layer, with decreasing TKED strength at depth (no profiles extended to the lake bottom, where higher dissipation rates would also be expected), demonstrating the stronger mechanical turbulence near the mixed layer. This is to be expected, as there was little wind during the deployments, and no significant current in the lake. Similarly, all profiles generally depict heightened thermal dissipation rates near the mixed layer, with decreasing TD strength far below. While this decrease in dissipation with increasing depth is clear in both TKED and TD rate profiles, the change is stronger in those of the thermal dissipation. The TD profiles also depict a trend not generally present in the TKED profiles: a significant decline in dissipation strength above the mixed layer, demonstrating the strongest thermal or "optical" turbulence resides near the thermocline, where the sharpest rate of change in the lake temperature profile occurs (Figure 2). While both dissipation rates demonstrate similar profile trends, the differences in magnitude and rate of change of the profiles with depth demonstrate the importance of measuring both in order to fully characterize the turbulent strength.

The two instrumental setups demonstrate reasonable agreement, with those of the Vector/CT tending to be higher in general than those of the VMP, as expected given the nature of the instrument setups, sampling rates, and estimate methods. Some deployment profiles demonstrate irregularities, however, again demonstrating the spatial and temporal variability of the turbulence field, and the difficulties this variability induces in quantifying the desired parameters. In Figure 6(a), for example, dissipation rates of both instruments span a wide range of values. The wide range of values is likely due to the significant drift experienced by both deployment vessels over the course of the deployment, showing the spatial and temporal changes in turbulent dissipation. However, the two vessels maintained close proximity of 5 to 10 m despite the drift, thus estimates from both instruments span the same range for most depths. Although the vessels drifted

less during the deployment shown in (b), proximity between the vessels was difficult to maintain, and separation was on the order of 50 to 100 m, which could account for the rather high estimates from the Vector/CT in comparison to the VMP, demonstrating the spatial variation in the turbulence field. Closer proximity of the two vessels (25 to 50 m) was maintained for the measurements shown in (c) and (d), although the vessels maintained a greater separation than on the first day shown in (a), and there was again significant drift during the course of the deployment for (c). Additional causes of the discrepancy between measurements could be attributed to the mounting of the Vector/CT within the IMAST structure for deployments (c) through (d), since it was mounted outside the optics cage in (a). Such mount design was mainly aimed to provide parameters for quantifying the turbulence impacts on imaging, rather than inter-comparison with the VMP.

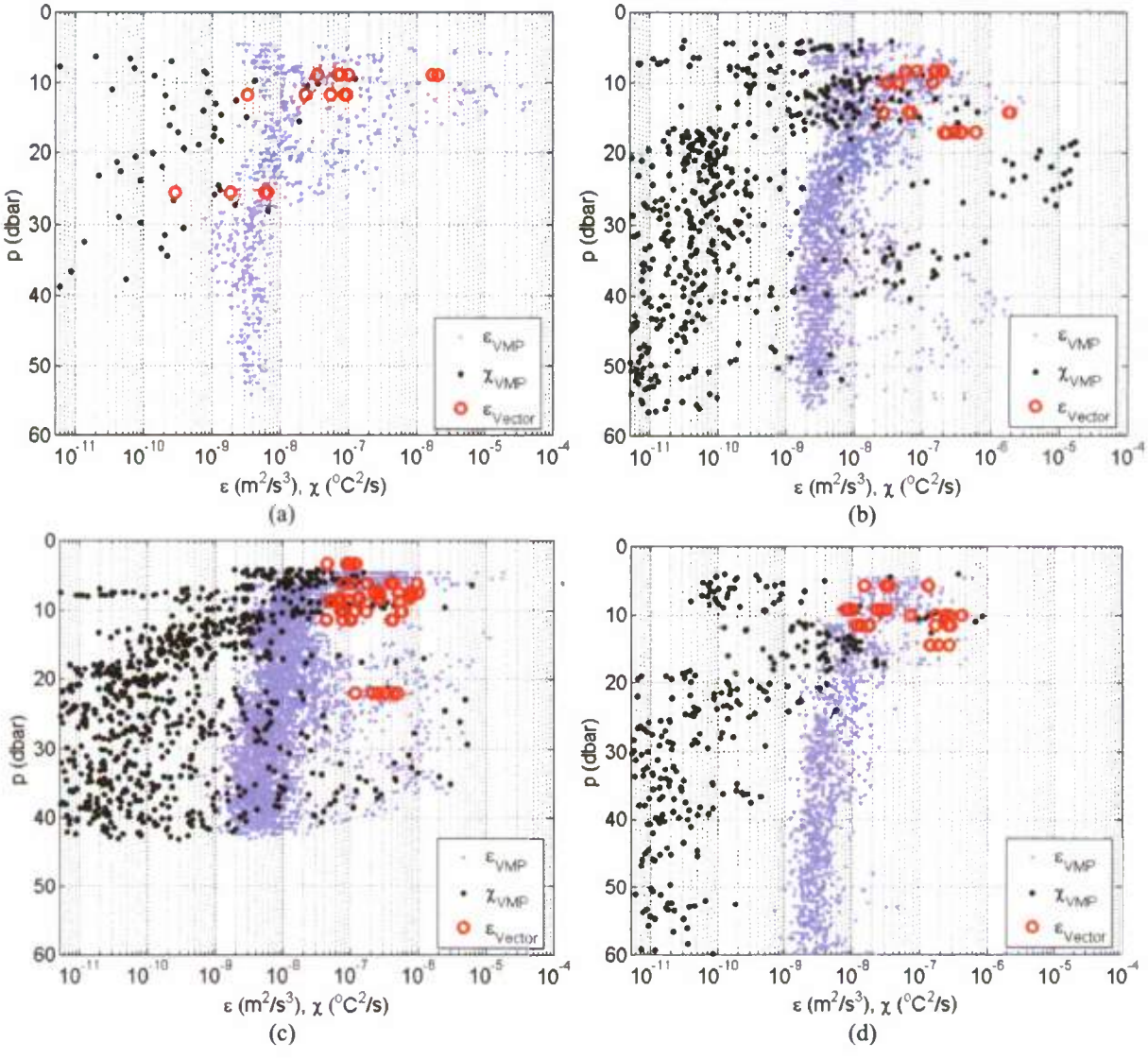

Figure 6. Profiles of turbulent kinetic energy dissipation rates, ε (m^2s^{-3}) determined from VMP (blue triangle) and Vector (red open circle) measurements, and thermal dissipation rates, χ ($°C^2s^{-1}$) determined from VMP (black dot) for several deployments: (a) July 27 daytime at S1, (b) July 28 daytime at S1, (c) July 29 daytime at S2, (d) July 29 nighttime at S1. The corresponding temperature profiles for each station are shown in Fig. 2. Note that in all cases the Vector/CT was on the IMAST except for (a), when it was on the optics package. Depth is given by pressure (dbar).

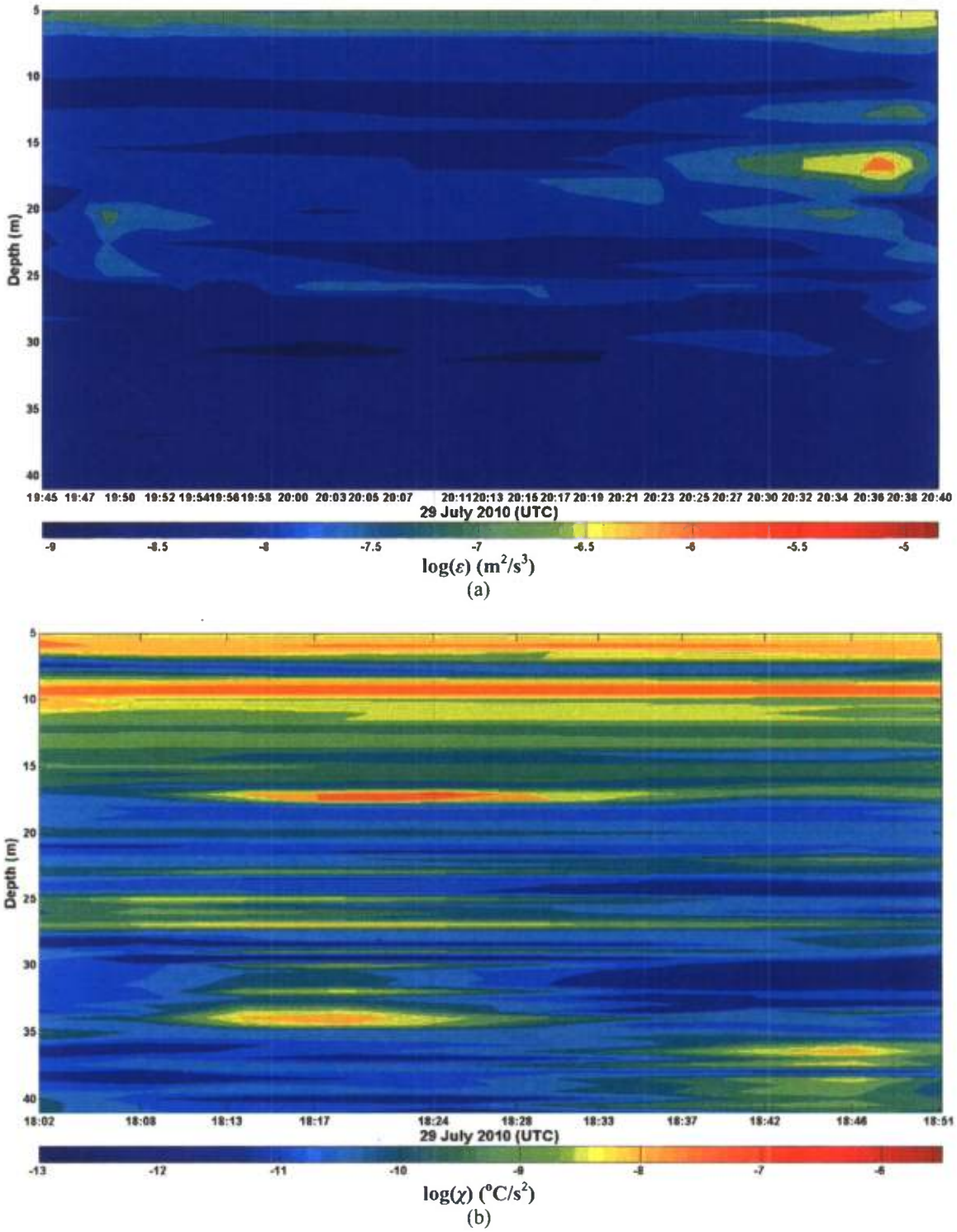

Figure 7. Interpolated VMP profiles of (a) TKED rate, ε (m^2/s^3), and (b) TD rate, χ ($°C/s^2$) showing the spatial and temporal variability of the turbulence field.

6. CONCLUSION

The Skaneateles Optical Turbulence EXercise (SOTEX), motivated by efforts to assess the impact of turbulence on underwater imaging, provided a unique opportunity to characterize the turbulent structure of the lake's water column, while also comparing turbulent characterization measurements from two rather different instruments: the Vector acoustic Doppler velocimeter and the Vertical Microstructure Profiler. Lake profiles of turbulent dissipation demonstrated the trend of stronger mechanical turbulence (as given by the kinetic energy dissipation rate) near the mixed layer, and stronger thermal (optical) turbulence (as given by the thermal dissipation rate) nearest the thermocline, as is expected given low wind and low current at the measurement site. The difference in profiles between the two dissipation rates demonstrated the importance of measuring both parameters for characterizing the turbulence strength. As for the instrument comparison, although the Vector is often deployed in a stationary moored setup, and the VMP in profile form, the two instruments demonstrated reasonable agreement in turbulent kinetic energy dissipation rate water column profiles when the two were deployed in close proximity. While some discrepancy exists, the disagreement between instruments can be attributed to proximity and drift of the deployment vessels and the spatial and temporal variability of the turbulence field. A better comparison could be made if these factors were eliminated. Such a deployment is difficult, however, due to the deployment needs of each instrument. Future work will further examine the agreement between the VMP and the Vector/CT through comparison of their estimated turbulent temperature dissipation rates and similar oceanic deployment of the two instruments.

ACKNOWLEGEMENTS

This work is sponsored by ONR/NRL program element 62782N (NRL core project 73-6369) and through the American Society for Engineering Education (ASEE). The authors thank the scientists and staff at the Upstate Freshwater Institute (UFI) for their assistance throughout SOTEX.

REFERENCES

[1] Hou, W., "A simple underwater imaging model," Opt. Lett. 34(17), (2009).
[2] Bogucki, D. J., Domaradzki, J. A., Stramski, D., and Zaneveld, J. R., "Comparison of near-forward light scattering on oceanic turbulence and particles," Appl. Optics 37(21), (1998).
[3] Woods, S., "Optical depolarization from turbulent convective flow: a laboratory study," Ph.D. dissertation, Division of Applied Marine Physics, University of Miami (2010).
[4] Hou, W., Woods, S., Goode, W., Jarosz, E., Weidemann, A., "Impacts of optical turbulence on underwater imaging," Ocean Sensing and Monitoring, Proc. Vol. 8030, SPIE Defense and Security Symposium, Orlando, FL, SPIE (2011).
[5] Wells, W. H., "Theory of small-angle scattering," Electromagnetics of the Sea (Advisory Group for Aerospace Research and Development, NATO, 92, Neuilly-Sur-Seine, France), (1973).
[6] Hodara, H., "Experimental results of small-angle scattering," Electromagnetics of the Sea (Advisory Group for Aerospace Research and Development, NATO, 92, Neuilly-Sur-Seine, France), (1973).
[7] Honey, R. C., and Sorensen, G. P., "Optical absorption and turbulence induced narrow-angle forward scatter in the sea," Electromagnetics of the Sea (Advisory Group for Aerospace Research and Development, NATO, 92, Neuilly-Sur-Seine, France), (1970).
[8] Bogucki, D. J., Domaradzki, J. A., Ecke, R. E., and Truman, C. R., "Light scattering on oceanic turbulence," Appl. Optics 43, 5662-5668, (2004).
[9] Kanaev, A. V., Ackerman, J., Fleet, E., and Scribner, D., "Imaging Through the Air-Water Interface," Computational Optical Sensing and Imaging (COSI), (2009).
[10] Hou, W., Gray, D. J., Weidemann, A. D., and Arnone, R. A., "Comparison and validation of point spread models for imaging in natural waters," Opt. Express 16(13), (2008).
[11] Hou, W., Gray, D. J., Weidemann, A. D., Fournier, G. R., and Forand, J. L., "Automated underwater image restoration and retrieval of related optical properties," IEEE 1889, (2007).
[12] Hou, W., Lee, Z., and Weidemann, A. D., "Why does the Secchi disk disappear? An imaging perspective," Opt. Express 15(6), (2007).

[13] Effler, S. W., Prestigiaeomo, A. R., and O'Donnell, D. M., "Water Quality and Limnologieal Monitoring for Skaneateles Lake: Field Year 2007," Upstate Freshwater Institute (2008).
[14] Tennekes, H., and Lumley, J. L., [A First Course in Turbulence], The MIT Press, Cambridge, (1972).
[15] Osborn, T. R., and Cox, C. S., "Oceanic fine structure," Geophys. & Astrophys. Fluid Dynam. 3(1), 321-345, (1972).
[16] Batchelor, G. K., "Small-scale variation in conveeted quantities like temperature in a turbulent fluid," J. Fluid Mcch. 5, 113-133, (1959).